THE JOURNAL OF PHYSICAL CHEMISTRY B

Article

pubs.acs.org/JPCB

Size- and Dimensionality-Dependent Thermodynamic Properties of Ice Nanocrystals

Y. Y. Han, J. Shuai, H. M. Lu,* and X. K. Meng*

College of Engineering and Applied Sciences, National Laboratory of Solid State Microstructures, Nanjing University, Nanjing 210093, P. R. China

ABSTRACT: Although the melting of ice is the most ubiquitous phase transition, (pre)melting and the quasi-liquid layer remain a matter of debate, and little is known about the relationship between the thermodynamic properties of ice nanocrystals and their size and dimensionality. Here, we model analytically the size- and dimensionality-dependent melting temperature, premelting temperature, and melting enthalpy of hydrogen-bonded ice nanocrystals. These three thermodynamic parameters are found to increase with increasing size and dimensionality where the size effect is principle while the dimensionality effect is secondary, and the size dependence of premelting temperature almost follows the same trend as that of melting temperature. The model predictions correspond to the available molecular dynamic simulation and experimental results of ice nanoparticles and nanowires. These agreements enable us to determine theoretically the thickness of the quasi-liquid layer for the first time, which is found to be not constant but slightly increase with increasing size and thus accounts for the occurrence of different reported thicknesses of the quasi-liquid layer.

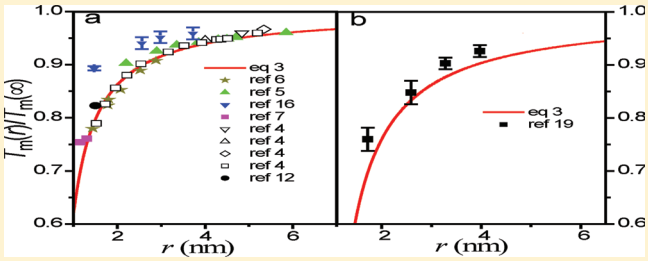

INTRODUCTION

The melting of ice is the most ubiquitous phase transition on Earth and plays a crucial role in our biosphere. In one of his famous Friday evening lectures held in 1850 at the Royal Institution in London, Faraday speculated as to whether the surface of ice is not solid but liquid even at temperature below 0 °C.[1] However, some 160 years or so later the premelting or quasi-liquid layer (QLL) remains a matter of debate and has been the subject of numerous recent experiments, molecular dynamics simulations, and thermodynamic theories.[2−26]

Unfortunately, it is difficult to prepare isolated ice nanocrystals in the laboratory.[8] Since nanopore materials with strictly ordered uniform cylindrical pores were synthesized in the 1990s,[2] many experiments have been carried out to study the melting processes of ice confined in the silica nanopores.[2−7] Given the interactions between ice nanocrystals and nanopore materials, they cannot be expected to display melting properties characteristic of isolated ice nanocrystals. In contrast with experiments, computer simulations as a useful tool to explore the melting process of isolated ice started about 40 years ago.[9,10] A key issue when performing simulations is the choice of the potential model used to describe the interaction between molecules. An excellent survey of the predictions of different models proposed up to 2009 was made by Vega et al.[11] However, they claimed that probably the general feeling was that no potential model was fully satisfactory.

It is well-known that the surface curvature affects the melting temperature where the dependence of the melting temperature T_m on the radius r has been linearly fitted by the modified Gibbs−Thomson equation[3,4]

$$T_m(r)/T_m(\infty) = 1 - \alpha V_s \gamma_{sl}/[H_m(r - t)] \quad (1)$$

where ∞ denotes the bulk; V_s is the molar volume of ice; γ_{sl} and H_m are the solid−liquid interfacial energy and the melting enthalpy of the bulk ice; and t is the thickness of the QLL, which does not appear in the original Gibbs−Thomson equation. α is a constant which depends on the topological structure of pores. For example, $\alpha = 3$ for spherical pores and 2 for cylindrical pores.[3]

Another major concern is surface premelting and the thickness of the QLL. However, to the best of our knowledge, there is no analytic expression proposed to describe the size dependence of premelting temperature T_p. On the other hand, although different values of t had been reported to range from 0.35 to 0.6 nm[5,12,13] which were usually determined through fitting experimental data with eq 1, this determination is indirect and relies on true (absolute) values of the pore size. Moreover, the theoretical attempt to determine the t value is also scarce.

Although eq 1 has been found to be valid for ice confined in ordered or disordered pores,[3,4,6] the inadequacy of this equation was also pointed out by some scientists, who found a deviation of the melting temperature from the linearity when the pore radius was less than ~1.5 nm.[2,14] These authors suggested that the temperature variations of V_s, γ_{sl}, and H_m should be taken into account.[14] Actually, the temperature effect on $\gamma_{sl}/H_m = \delta/a_m$ had already been discussed by Turnbull

Received: November 29, 2011
Revised: January 11, 2012
Published: January 17, 2012

where δ is a constant and a_m denotes the surface area per atom.[27] In other words, the temperature dependences of V_s, γ_{sl}, and H_m are largely compensated by each other in the Gibbs–Thomson equation. This behavior may be one of the reasons why the parameters taken from normal conditions can be successfully used even in the supercooled state.

On the other hand, melting enthalpy H_m of nanocrystals has also been found to vary with the size.[2,13,28−30] Assuming that the melting enthalpy was attributed solely to the amount contained in the core of the pores, the size-dependent melting enthalpy $H_m(r)$ had been linearly fitted by the following equation[13]

$$H_m(r)/H_m(\infty) = 1 - \chi/(r - t) \quad (2)$$

where $\chi = 0.75 \pm 0.02$ nm and $t = 0.6$ nm were determined through fitting the experimental results with eq 2,[13] while other experiments gave $t = 0.38$ nm.[2] Thus, it is necessary to develop a quantitatively thermodynamic analytic model to determine the size dependence of the melting enthalpy and deepen our understanding of its nature.

In this work, a size-dependent melting temperature model originally proposed for metallic nanocrystals has been extended to describe the size and dimensionality dependences of melting temperature, premelting temperature, melting enthalpy, and thickness of the QLL of hydrogen-bonded ice nanocrystals through considering the effect of positional entropy.

METHODOLOGY

On the basis of the size-dependent amplitude of the atomic thermal vibrations in nanocrystals and the Lindemann's melting criterion, a size- and dimensionality-dependent melting temperature model for metallic nanocrystals has been proposed as[31]

$$\frac{T_m(r, d)}{T_m(\infty)} = \exp\left[- \frac{2S_{vib}}{3R} \frac{1}{r/r_0(d) - 1} \right] \quad (3)$$

where R is the ideal gas constant; S_{vib} is the vibrational component of the melting entropy; and r_0 is a critical radius at which all atoms of particles located on its surface. The critical radius r_0 has been determined as $r_0 = (3 - d)h$ with d and h being the dimensionality and the atomic diameter or nearest molecular distance.[32] It is known that hexagonal ice at ambient conditions can be thought of as a stack of crystalline planes on which the oxygen atoms display a perfect hexagonal arrangement. Since the mean distance between adjacent H_2O molecules is 0.276 nm,[15] there is $h = 0.276$ nm according to its definition.

Usually, the melting entropy S_m consists of three contributions:[32] positional S_{pos}, vibrational S_{vib}, and electronic S_{el}. Namely, $S_m \approx S_{vib} + S_{el} + S_{pos}$ and $S_{pos} = -R \ln(x_A \ln x_A + x_B \ln x_B)$, where x_A and x_B are molar fractions of crystals and vacancies and $x_A + x_B = 1$.[32] If the type of chemical connection does not vary during the melting transition, e.g., for metals and ice, the electronic component S_{el} is negligible. For the melting transition, $x_A = 1/(1 + \Delta V/V_s)$, with ΔV being the absolute value of volume change during the transition. Due to the small volume change ΔV, the S_{pos} of metals is also apparently small in comparison with S_m. As a result, S_m for metals is mainly vibrational in nature, and $S_{vib} \approx S_m$ is usually used.[31] However, for ice crystal, the large volume change during the transition makes S_{pos} not negligible and thus

$$S_{vib} \approx S_m - S_{pos} \quad (4)$$

According to the classic thermodynamics, there is $H_m = T_m S_m$. When the nanocrystals have the same structure of the corresponding bulk, this expression may be extended to nanometer size with the same form, namely, $H_m(r) = T_m(r) S_m(r)$. Combining eq 3 and the size-dependent melting entropy $S_m(r)$ function reported in ref 31, one can obtain the size- and dimensionality-dependent melting enthalpy $H_m(r,d)$ as

$$\frac{H_m(r, d)}{H_m(\infty)} = \left[1 - \frac{1}{r/r_0(d) - 1} \right] \exp\left[- \frac{2S_{vib}}{3R} \frac{1}{r/r_0(d) - 1} \right] \quad (5)$$

As we know, the occurrence of melting or premelting means that the bonding of interior or surface atoms is destroyed. Since the melting temperature is linear to the cohesive energy of interior atoms based on Lindemann's criterion of melting,[33] the premelting temperature should thus be proportional to the cohesive energy of surface atoms. The reason why premelting temperature T_p is lower than melting temperature T_m mainly results from the deficiency of coordination number of surface atoms in comparison with interior atoms.[34] The energetic difference between surface and interior atoms is the surface energy or interface energy, which has been deduced to be linearly proportional to cohesive energy of interior atoms.[28] As a result, it can be concluded that the dependences of premelting temperature on nanocrystal size and dimensionality should also follow the trend same as those of cohesive energy and melting temperature. Namely

$$\frac{T_p(r, d)}{T_p(\infty)} \approx \exp\left[- \frac{2S_{vib}}{3R} \frac{1}{r/r_0(d) - 1} \right] \quad (6)$$

RESULTS AND DISCUSSION

On the basis of eq 1 with $d = 1$, Figure 1a shows the calculated $T_m(r)$ functions of ice nanowires (the solid line). It is obvious that the melting temperature of ice nanowires decreases with reducing size, and the drop becomes dramatic at $r < 3$ nm. Note

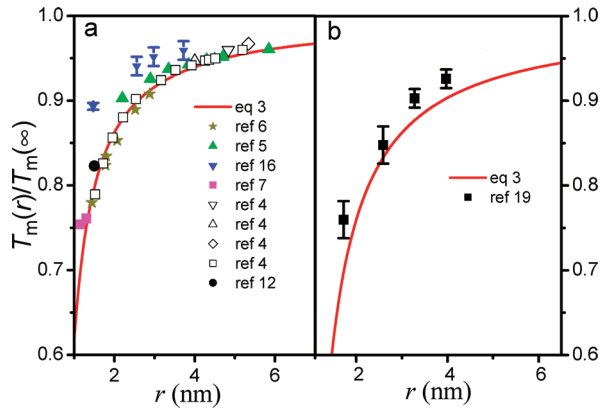

Figure 1. Normalized temperature $T_m(r)/T_m(\infty)$ functions of ice (a) nanowires and (b) nanoparticles where the solid lines are plotted based on eq 3 where the symbols correspond to available experimental data[4−7] and simulation results.[12,16,19] $S_m = H_m/T_m \approx 7.35$ J/g atom K,[11] and $\Delta V/V_s = (\rho_l - \rho_s)/\rho_l \approx 8.2\%$ with ρ_l and ρ_s being the density of water and hexagonal ice,[11] and thus $S_{vib} \approx 4.99$ J/g atom K in terms of eq 4.

dx.doi.org/10.1021/jp211469e | J. Phys. Chem. B 2012, 116, 1651–1654

that hydrogen bonds are the dominant interactions between H_2O molecules, and the strength of the bond is large enough so that the melting temperature and melting enthalpy of the system are strongly dependent on the average number of bonds broken in the network.[22,24] Since the hydrogen bond strength decreases with reducing system size,[22] the depression of $T_m(r)$ for ice nanowires is thus understandable. As a comparison, available molecular dynamics simulation results[12,16] and experimental data[4−7] are also listed where good agreements between our model predictions and the corresponding molecular dynamics simulation results or experimental data can be found. Note that the data[4−7,12] correspond to ice nanowires confined in silica nanopores. While the interaction between silica nanopores and ice nanowires is not included in our model, the agreements shown in Figure 1a indicate that the effect of this interaction on the melting temperature depression is small and thus negligible as a first-order approximation. Actually, this neglect is feasible since the density of the OH bonds on the surface of the pore wall of silica nanopores is only a tenth of that on the surface of ice nanocrystals, and thus most of the molecules on the surface of ice are free of chemical interaction with the nanopore walls.[17,18] Moreover, the agreements shown in Figure 1a also reveal that the change in ice−nanopore interactions has an extremely weak effect on the melting temperature reduction, with the note that the acid-functionalized SBA-15 nanopore walls in the experiments[4] were decorated with carboxylic, phosphonic, and sulfonic acids, respectively.

Figure 1b compares the $T_m(r)$ function of ice nanoparticles between the model prediction in terms of eq 3 with $d = 0$ and available molecular dynamics simulation results[19] where reasonable agreements can also be found. Because it is difficult to prepare isolated ice nanocrystals in the laboratory, there is no comparison between our model predictions and the corresponding experimental results. As shown in Figure 1, $T_m(r)$ values of ice nanoparticles at the same size are always smaller than those of ice nanowires, which indicates that the size effect on the melting temperature in ice nanoparticles is more prominent than that in nanowires. Moreover, in a more general sense, the agreements shown in Figures 1a and 1b confirm that the size-dependent melting temperature model (i.e., eq 3) originally established for metallic nanocrystals is also applicable to hydrogen-bonded ice nanocrystals.

Noting that $\exp(-x) \approx 1 - x$ when x is small enough (e.g., $x < 0.1$ or $r > 5r_0$), eq 3 can be simplified as

$$T_m(r, d)/T_m(\infty) \approx 1 - 2(3 - d)S_{vib}h/(3Rr) \quad (7)$$

It is evident that the melting temperature decreases with reducing size and dimensionality. Given that d only ranges from 0 to 2 while r can vary from r_0 to several tens of nanometers, it suggests that the size effect is principle and the dimensionality effect is secondary. Moreover, based on eq 7 with $d = 0$ for nanoparticles and 1 for nanowires, the ratio of the melting temperature depression between ice nanoparticles and nanowires is 3:2 at $r > 5r_0$, which is the same as the prediction of eq 1 where $\alpha = 3$ for spherical pores and 2 for cylindrical pores.[3] Note that h for metal is similar to that for ice, and $S_{vib}/R \approx 1.1$ for metal and 0.6 for ice. As a result, metal nanocrystals usually exhibit more dramatic depression in melting temperatures with crystal size than that in ice according to eq 7.

Figure 2 shows the comparison of the $T_P(r)$ function of ice nanoparticles between the model calculation in terms of eq 5 and available molecular dynamics simulation results[19] where

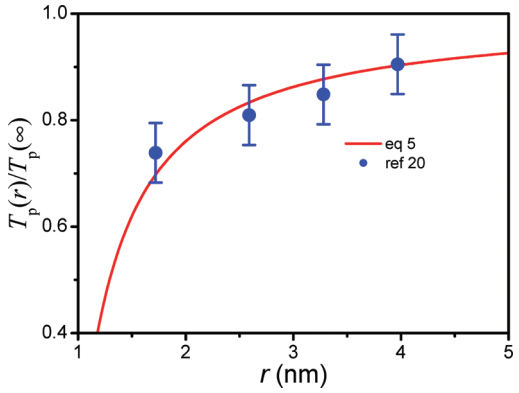

Figure 2. Comparison of normalized temperature $T_P(r)/T_P(\infty)$ of ice nanoparticles described by eq 5 and molecular dynamics simulation results.[19]

good agreements can also be found, which indicates that the dependence of premelting temperature on size indeed follows the same trend as that of melting temperature as a first-order approximation.

The melting enthalpy of ice nanowires determined by eq 6 is shown in Figure 3 (the solid line). It can be found that $H_m(r)$

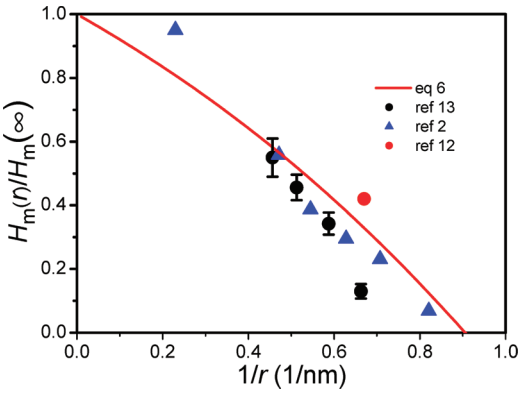

Figure 3. Comparison of normalized enthalpy $H_m(r)/H_m(\infty)$ of ice nanowires described by eq 6 and molecular dynamics simulation results[12] as well as experimental data.[2,13]

almost drops linearly with increasing $1/r$ at $1/r < 0.4$ nm^{-1}, which agrees with the general consideration that the change of any size-dependent thermodynamic parameter is proportional to $1/r$ where only the effect of surface atoms is considered.[35] However, when $1/r$ increases further, the melting enthalpy depression based on eq 6 is larger than the above-mentioned linear depression, which is because interior atoms should also have a contribution on the $H_m(r)$ depression besides surface atoms. As a comparison, available molecular dynamics simulation results[12] and experimental data[2,13] are also listed where good agreements can be found.

In the experiment,[13] it is found that the melting/freezing hysteresis disappears when the cylindrical pore size is small enough, which indicates that melting and freezing as a true first-order phase transition occur only above a minimum pore size. On the basis of eq 6, the melting enthalpy reaches zero when $r = 2r_0$. Thus, the minimum cylindrical pore radius is $4h \approx 1.1$ nm for ice nanowires, which is close to a phenomenological model prediction of 1.2 nm[20] but smaller than the differential scanning calorimetric measurement result of 1.4 ± 0.05 nm.[13]

dx.doi.org/10.1021/jp211469e | J. Phys. Chem. B 2012, 116, 1651−1654

The agreements shown in Figure 3 indicate that eq 6 can satisfactorily describe the size-dependent melting enthalpy of ice. Since it is claimed that eq 2 can also be employed to model $H_m(r)$ functions of ice nanowires, the combination of eq 2 with eq 6 can be used to determine the thickness of QLL. Namely

$$t(r) = r - \chi/\left[1 - \left(1 - \frac{1}{r/r_0 - 1}\right) \exp\left(-\frac{2S_{vib}}{3R}\frac{1}{r/r_0 - 1}\right)\right] \quad (8)$$

The thickness of the QLL determined by eq 8 for ice nanowires is shown as a function of radius in Figure 4. It is

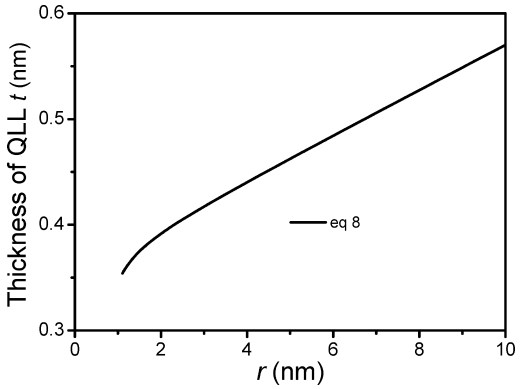

Figure 4. Thickness of the QLL as a function of size based on eq 8 for ice nanowires.

observed that t increases with increasing r where the slope is very small (only about 0.02). According to eq 8, the minimum value of QLL thickness for ice nanowires can be determined to be $t_{min} = t(r \to 2r_0) \approx 2r_0 - \chi = 0.35$ nm. When the radius of cylindrical nanopores is in the range of 1.1−10 nm which is the size range usually employed in the simulation and experiments, our calculated t value increases from 0.35 to 0.57 nm, which corresponds to the reported 0.35 ± 0.04, 0.38 ± 0.06, and 0.6 ± 0.01 nm.[5,12,13]

CONCLUSIONS

In summary, a size-dependent melting temperature model originally proposed for metallic nanocrystals has been extended to describe the size and dimensionality dependences of melting temperature, premelting temperature, and melting enthalpy of hydrogen-bonded ice nanocrystals through including the effect of positional entropy. The three thermodynamic parameters are found to increase with increasing size and dimensionality where the size effect is principle while the dimensionality effect is secondary. The model predictions correspond to the available molecular dynamics simulation and experimental results, which enable us to determine theoretically the thickness of the quasi-liquid layer for the first time. The thickness is not constant but increases with increasing size with a slope of 0.02, which may be the cause of different reported t values in different literatures.

AUTHOR INFORMATION

Corresponding Author

*Phone: +86-025-8368-5585. Fax: +86-025-8359-5535. E-mail: haimlu@nju.edu.cn and mengxk@nju.edu.cn.

Notes

The authors declare no competing financial interest.

ACKNOWLEDGMENTS

This work was jointly supported by the FANEDD, PAPD, the Fundamental Research Funds for the Central Universities, the National Natural Science Foundation of Jiangsu, the Program for New Century Excellent Talents in University, the National Natural Science Foundation of China, and the State Key Program for Basic Research of China.

REFERENCES

(1) Faraday, M. *Faraday's Diary*; Bell and Sons: London, 1933.
(2) Kittaka, S.; Ishimaru, S.; Kuranishi, M.; Matsuda, T.; Yamaguchi, T. *Phys. Chem. Chem. Phys.* **2006**, *8*, 3223.
(3) Liu, X. X.; Wang, Q.; Huang, X. F.; Yang, S. H.; Li, C. X.; Niu, X. J.; Shi, Q. F.; Sun, G.; Lu, K. Q. *J. Phys. Chem. B* **2010**, *114*, 4145.
(4) Findenegg, G. H.; Jähnert, S.; Akcakayiran, D.; Schreiber, A. *Chem. Phys. Chem.* **2008**, *9*, 2651.
(5) Schreiber, A.; Ketelsen, I.; Findenegg, G. H. *Phys. Chem. Chem. Phys.* **2001**, *3*, 1185.
(6) Morishige, K.; Kawano, K. *J. Chem. Phys.* **1999**, *110*, 4867.
(7) Deschamps, J.; Audonnet, F.; Brodie-Linder, N.; Schoeffel, M.; Alba-Simionesco, C. *Phys. Chem. Chem. Phys.* **2010**, *12*, 1440.
(8) Hock, C.; Schmidt, M.; Kuhnen, R.; Bartels, C.; Ma, L.; Haberland, H.; von Issendorff, B. *Phys. Rev. Lett.* **2009**, *103*, 073401.
(9) Barker, J. A.; Watts, R. O. *Chem. Phys. Lett.* **1969**, *3*, 144.
(10) Rahman, A.; Stillinger, F. H. *J. Chem. Phys.* **1971**, *55*, 3336.
(11) Vega, C.; Absacal, J. L. F.; Conde, M. M.; Aragones, J. L. *Faraday Discuss.* **2009**, *141*, 251.
(12) Moore, E. B.; de la Llave, E.; Welke, K.; Scherlis, D. A.; Molinero, V. F. *Phys. Chem. Chem. Phys.* **2010**, *12*, 4124.
(13) Jähnert, S.; Chavez, F. V.; Schaumann, G. E.; Schreiber, A.; Schonhoff, M.; Findenegg, G. H. *Phys. Chem. Chem. Phys.* **2008**, *10*, 6039.
(14) Tombari, E.; Salvetti, G.; Ferrari, C. *J. Chem. Phys.* **2005**, *122*, 104712.
(15) Dosch, H.; Lied, A.; Bilgram, J. H. *Surf. Sci.* **1996**, *366*, 43.
(16) Pereyra, R. G.; Carignano, M. A. *J. Phys. Chem. C* **2009**, *113*, 12699.
(17) Jiang, Q.; Liang, L. H.; Zhao, M. *J. Phys.: Condens. Matter* **2001**, *13*, 397.
(18) Hansen, E. W.; Stöcker, M.; Schmidt, R. *J. Chem. Phys.* **1996**, *100*, 2195.
(19) Pan, D.; Liu, L. M.; Slater, B.; Michaelides, A.; Wang, E. *ASC Nano* **2011**, *5*, 4562.
(20) Denoyel, R.; Pellenq, R. J. M. *Langmuir* **2008**, *18*, 2710.
(21) Johari, G. P. *J. Chem. Phys.* **1998**, *109*, 1070.
(22) Ludwig, R. *Angew. Chem., Int. Ed.* **2001**, *40*, 1808.
(23) Richardson, H. H.; Thomas, A. C.; Carlson, M. T.; Kordesch, M. E.; Govorov, A. O. *J. Electron. Mater.* **2007**, *36*, 1587.
(24) Fernández-Serra, M. *Physics* **2009**, *2*, 67.
(25) Levitas, V. I.; Samani, K. *Nature Commun.* **2011**, *2*, 284.
(26) Guisbiers, G. *J. Nanosci. Lett.* **2012**, *2*, 8.
(27) Turnbull, D. *J. Appl. Phys.* **1950**, *21*, 1022.
(28) Jiang, Q.; Lu, H. M. *Surf. Sci. Rep.* **2008**, *63*, 427.
(29) Liang, L. H.; Zhao, M.; Jiang, Q. *J. Mater. Sci. Lett.* **2002**, *21*, 1843.
(30) Guisbiers, G.; Buchaillot, L *J. Phys. Chem. C* **2009**, *113*, 3566.
(31) Jiang, Q.; Tong, H. Y.; Hsu, D. T.; Okuyama, K.; Shi, F. G. *Thin Solid Films* **1998**, *312*, 357.
(32) Regel', A. R.; Glazov, V. M. *Semiconductors* **1995**, *29*, 405.
(33) Tateno, J. *Solid State Commun.* **1972**, *10*, 61.
(34) Shidpour, R.; Delavari, H. H.; Vossoughi, M. *Chem. Phys.* **2010**, *378*, 14.
(35) Jiang, Q.; Shi, H. X.; Zhao, M. *J. Chem. Phys.* **1999**, *111*, 2176.